Hindawi
International Journal of Photoenergy
Volume 2022, Article ID 2845755, 9 pages
https://doi.org/10.1155/2022/2845755

Research Article

A Machine Learning-Based Novel Energy Optimization Algorithm in a Photovoltaic Solar Power System

Kalapala Prasad,[1] J. Samson Isaac,[2] P. Ponsudha,[3] N. Nithya,[4] Santaji Krishna Shinde,[5] S. Raja Gopal,[6] Atul Sarojwal,[7] K. Karthikumar,[8] and Kibrom Menasbo Hadish[9]

[1]*Department of Mechanical Engineering, University College of Engineering Kakinada, JNTUK, Kakinada, Andhra Pradesh 533003, India*
[2]*Department of Biomedical Engineering, Surgical and Critical Care Equipment Laboratory, Karunya Institute of Technology and Sciences, Coimbatore, Tamil Nadu 641114, India*
[3]*Department of Electronics and Communication Engineering, Velammal Engineering College, Chennai, Tamil Nadu 600066, India*
[4]*Department of Electronics and Communication Engineering, Panimalar Engineering College, Chennai, Tamil Nadu 600123, India*
[5]*Computer Engineering Department, Vidya Pratishthan's Kamalnayan Bajaj Institute of Engineering & Technology, Baramati, Maharashtra 413133, India*
[6]*Department of Electronics & Communications Engineering, Koneru Lakshmaiah Education Foundation, Vaddeswaram, Andhra Pradesh 522502, India*
[7]*Department of Electrical Engineering, FET, MJP Rohilkhand University, Bareilly, Uttar Pradesh 243006, India*
[8]*Department of Electrical and Electronics Engineering, Vel Tech Rangarajan Dr. Sagunthala R&D Institute of Science and Technology, Avadi, Chennai, Tamil Nadu 600062, India*
[9]*Faculty of Mechanical Engineering, Arba Minch University, Arba Minch, Ethiopia*

Correspondence should be addressed to Kibrom Menasbo Hadish; kibrom.menasbo@amu.edu.et

Received 4 June 2022; Revised 2 September 2022; Accepted 8 September 2022; Published 28 September 2022

Academic Editor: BR Ramesh Bapu

Performance, cost, and aesthetics are all difficult to beat in today's expanding distributed rooftop solar sector, and flat-plate PV is no exception. Photovoltaics will be able to take advantage of some of their most significant advantages as a result of this marketplace, including the elimination of transmission losses and the generation of power at the point of sale. Concentrated photovoltaic (CPV) technology, on the other hand, represents a viable alternative in the quest for ever-lower normalised energy costs and ever-shorter energy payback times. Material, components, and manufacturing techniques from allied sectors, particularly the power electronics industry, have been adapted to lower system costs and time-to-market for the system under development. The LFR is less than 30 mm wide to maximise thermal efficiency, and a densely packed cell array has been used to maximise electrical output. The Matlab simulations show that the proposed machine learning-based LFR technique has a greater concentration rate than the present LFR method, as demonstrated by the results.

1. Introduction

The usage of distributed energy resources (DERs) including solar power and wind has increased dramatically around the world in recent years [1, 2]. Furthermore, solar energy is a completely free, easily accessible, and scalable renewable resource that may be used in a variety of applications and shown in Figure 1 [3]. The utilisation of solar panels to generate considerable amounts of electricity without the use of fossil fuels will enable the world to transition to a clean energy economy. Several international rules and financial incentives have been implemented to increase solar energy share in the smart grid [4]. It will be difficult for photovoltaic (PV) power plants to expand on a large scale if there is

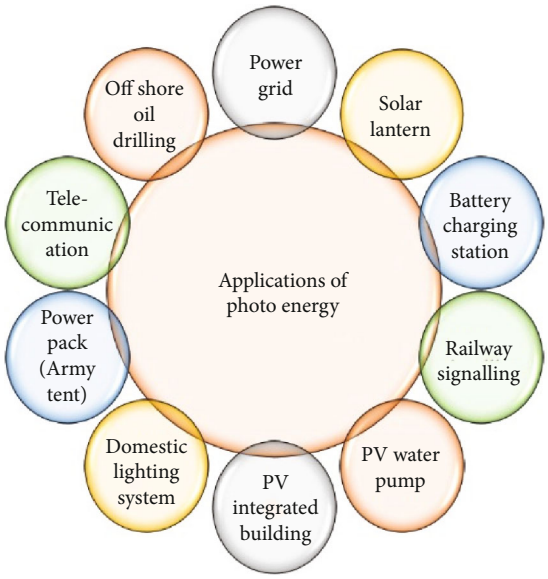

Figure 1: Shows applications of photo energy.

uncertainty in the real-time control and economic benefits they provide. To mitigate the negative effects of PV power on the overall power system and to improve system stability, it has become more important to employ reliable forecasting methods for precisely anticipating PV power [5, 6]. The utilisation of more detailed source data can be utilised to develop more advanced forecasting models, which can then be used to attain an increased average accuracy rate of PV power forecasts using the current power grid smart electricity metres [7].

It was impossible to design a high-efficiency solar energy conversion system long ago while keeping costs down. Using normal methods, it is difficult to evaluate and predict the heat transfer and storage characteristics of a typical solar energy conversion device, such as a solar water heater (SWH) [8]. For the high-performance SWH design, it is vital to be familiar with the relationships that exist between external settings and thermal performance coefficients (CTP). On the other hand, some relationships are challenging to understand for a number of reasons, including [9]. Measurements take time, control experiments are found difficult for conducting, and currently, no model adequately integrates external settings with inherent SWH properties. Methods for assessing energy system attributes [10, 11] and enhancing system performance [12–15] are currently at the forefront of technological development. Although there are certain exceptions to this rule, there are a few. Due to these challenges, as well as cost constraints, the logical design of high-performance SWHs is significantly hampered.

The fact that machine learning assists us in precisely determining the values of CTP with only a few easily measured independent variables is fortunate for us. Using a nonlinear fitting approach and a machine learning technique with proper algorithms, assuming the database is large enough to learn from the correlations in the data, this can be accomplished with relative ease. Using this technique, we can obtain a prediction from the predictive model without having to determine the unique physical models for each CTP. As these research findings illustrate, machine learning technologies have a great deal of potential in the field of energy systems. Power systems are complex, dynamic networks of electrical components that operate in a dynamic environment. The evolution of electricity systems has occurred over several decades. Economic, technological, environmental, and political motivations have all played a role in bringing about these transformations [1–3]. In a smart grid system [4, 5], both energy and information are sent back and forth amongst the numerous stakeholders, allowing for bidirectional energy flow as well as bidirectional information flow. Several factors have contributed to the disruption of the energy system. As a starting point, the rising reliance on renewable energy sources by the power system introduces greater uncertainty. Identifying solutions that allow for the adoption of distributed energy resources in a deregulated electricity market becomes more difficult as customers become more involved in the market [6, 7].

To address these concerns, effective grid planning and operating procedures are required. As a result of the ongoing grid changes [8, 9], both commercial transactions and the physical flow of electricity are becoming increasingly complex. Because of the abundance of data and the instability of information, decision-making has become more difficult than it used to be [10, 11]. Future smart grids will consequently necessitate the development of systems that can continuously monitor, predict, and schedule energy consumption and output in real-time, as well as learn and make decisions.

2. Related Works

Many power system challenges can be broken down into a set of sequential decisions that must be made one after another. Traditional methods include things like programming, convex optimization, and heuristic approaches, to name a few. The advantages and disadvantages of these methods can be better understood by contrasting them with optimisation algorithms on a qualitative level [16, 17]. The mathematical approach known as Lyapunov optimization is an example of a classical mathematical approach [18]. There are several advantages to this strategy, including exact mathematics and real-time management. Because it is based on explicit objective functional expressions, it cannot be used to abstract away many real-world optimization option scenarios from the optimization problem [19]. The validity of the Lyapunov criterion in complicated, high-dimensional settings is also in doubt, according to some researchers.

For any programming style, such as mixed-integer programming, dynamic programming, or stochastic programming, there are a variety of options to choose from. These strategies can be used for a variety of problems, including sequence optimization problems [20–25]. Despite this, it is required to start over with each iteration of this strategy because the results are so complex. Aside from that, the expense of computation makes real-time decision-making impractical in some circumstances. It is difficult to effectively

predict renewable energy generation and demand in real-world situations using computer-aided forecasting techniques [26–30]. In the field of heuristic techniques, particle swarm optimization (PSO) [31, 32] and genetic algorithms (GA) [33, 34] are two examples. The application of a heuristic technique to address optimization problems, particularly nonconvex optimization problems, is effective in dealing with the challenge of large data sets and complex situations. However, because they cannot be quantitatively verified, these procedures are less dependable than other alternatives [35]. It is not necessary to have an exact objective function when using machine learning techniques, as is the case with convex optimization approaches. For its part, machine learning examines the decision-making process in the context of the data that is fed into it. While convex optimization approaches have problems dealing with huge datasets, machine learning does not have this problem. The major importance of the proposed machine learning-based approach is to produce the solar power optimization in the automatic. Hence, there is the result, and computational accuracy was increased. If these attributes get higher values, then, the results are getting huge. So the machine learning model was introduced in power optimization. The current status of the system indicates that machine learning generates online decisions in real time rather than relying on a set of rules that have been established in advance. Machine learning, in contrast to heuristic methods, is more stable and better suited for decision-making tasks than these methods.

3. Background

To focus sunlight onto a stationary absorber, Fresnel reflectors with long, thin segments use a shared focal point. Using a secondary concentrator, the beams are reflected within the accepted angle of incidence. The absorber is responsible for converting this concentrated energy into the thermic fluid. Power or other commercial reasons can be generated through the use of a heat exchanger. The LFRSC modular components can be joined together to form a bigger system, depending on the application being addressed. A rooftop collector is built with Fresnel mirrors and a secondary concentrator with CPCs, which we used in conjunction with the linear Fresnel reflecting mirrors. The PRO-e Package is used to represent the collector assembly and the components that make up the assembly. Radiation from the beam is focused on a stationary receiver employing Fresnel reflectors. The receiver is made up of two absorber tubes made of stainless steel. Secondary CPC reflectors on receivers direct beam radiation to the absorber tube, which serves as the receiver receiving element. A thick pane of glass protects the entire optical system from exposure to the outside environment.

Its dimensions are 2.2 metres in length, 1.383% in width, and 0.351% in height, and it weighs 0.351 kilogrammes. Each mirror array in the CPC system is made up of ten mirrors, which is the maximum number allowed. The sunlight is focused onto two parallel tubes of absorber by a total of twenty mirrors with similar widths. The receiver is made up of two absorber tubes made of stainless steel with a diameter of 25 mm. When it comes to optical design, the angle of incidence of the reflecting mirror is considered crucial. Thin mirrors are often utilised to focus on the absorber at the shared focal point of the reflector and the reflector absorber. Reflected radiation from the neighbouring mirrors should not be hindered by the space between them if they are placed close together. As a result, there is no mirror placed beneath the absorber to prevent the shadow generated by this device and the secondary concentrator. When estimating the radii of tube absorbers, the perpendicular drop lengths from point f on reflector rays are taken into consideration. To design the LFRSC, the tubular absorber served as a starting point for the process [1]. The tubular absorber radius can be approximated as half the width of the mirror element [2] divided by its radius. In this case, the first mirror is located $0.5W + f \tan(\xi_0)$ distance from the planes, whereas the second mirror is located at $0.5W$ distance. Values larger than one-half the length of the mirror should be avoided at all costs. As a result, shading will not be provided. The study refers to the first mirror element as Q_1 in Equation (1) for the time being.

$$Q_1 = R + f \tan(\xi_0), \tag{1}$$

where Q_1 is the first mirror location, R is the absorber radius, and f is the focal distance.

The first mirror element inclination is shown below:

$$\theta_1 = 0.5\left[\frac{(Q_1 + (0.5W)\cos\theta_1)}{(f - (0.5W)\sin\theta_1)}\right]. \tag{2}$$

Upon impacting the second mirror element, its positioning and tilt concerning the aperture plane are adjusted to ensure that it will arrive at its focal point in the proper position. As a result, the first and second mirrors require some more breathing room. As a result, the second mirror shift is referred to as the shift. The second mirror is beginning to shift as in the following equation:

$$S_2 = W \sin\theta_1 \tan(2\theta_2 + \xi_0). \tag{3}$$

The position and tilt of the second mirror w.r.t the aperture plane are critical factors as in the following equation:

$$\left(XX'\right) \text{ is } Q_2 = Q_1 + W\cos\theta_1 + S_2. \tag{4}$$

Generalized equations for the location of shift (S) and its tilt of the n^{th} mirror are obtained using geometrical considerations that are similar to those used in the previous formulations in the following equations:

$$\begin{aligned} Q_n &= Q_{n-1} + W\cos\theta_{n-1} + S_n, \\ S_n &= W\sin\theta_{n-1}\tan(2\theta_n + \xi_0), \\ \theta_n &= 0.5\left[\frac{(Q_n + (0.5W)\cos\theta_n)}{(f - (0.5W)\sin\theta_n)}\right], \end{aligned} \tag{5}$$

With $S_1 = 0$, $\theta_1 = 0$, and $Q_1 = 0.5\,\mathrm{W} + f\ \tan(\xi_0)$ are considered as the initial values for the optimisation process, and the value of n varies between 1 and K, where K is the number of mirrors elements found at either half of the parabolic concentrators. Shift, tilt, and location can be calculated using the iteration method by calculating the equations above for each mirror element. A total of 20 mirror components are required for a complete module with two absorbers. The secondary concentrator profile is designed based on the relationships shown in the following equations:

$$\begin{aligned} R &= \frac{2f}{(1-\cos\phi)}, \\ z &= R\cos(\phi - \theta_{\max}), \\ r &= R\sin(\phi - \theta_{\max}) - a', \\ f_l &= a'(1-\cos(90+\theta_{\max})), \\ 2a' &= \frac{2f}{(1-\cos(90+\theta_{\max}))}, \end{aligned} \tag{6}$$

where f_l is the parabola, $\theta_{\max}$ is the focal length, $2a^{'}$ is the acceptance angle, z is the spherical coordinate, and r is the absorber radius.

4. Proposed Method

With a linear Fresnel reflector (LFR) tracking in the north-south direction, it was thought that the reflector would be able to produce a level of performance that would be acceptable. Because the collector design is the primary focus of this study, it is critical to determine the maximum power output that can be achieved for a certain operational surface temperature of the absorber pipe. The machine learning was supported for automation predictions and optimization. Hence, the reduction of human level was possible. So the optimization will get accurate results while the manual calculations. The proposed model operates on the Carnot cycle. The Carnot cycle eliminates the need to make assumptions regarding piping configuration, flow rate, or the heat engine or heat transfer fluid that would be required to model a complete plant. Even though the energy approach has significant disadvantages, it is still extensively employed in the solar literature, despite the thought taking into account specific applications. The TMY hourly average of energy per unit area (in $\mathrm{W/m^2}$ of the total mirror area of the collector) for an LFR is calculated as follows:

$$E_{x,\mathrm{out}} = Q\left(1 - \frac{T_a}{T_r}\right), \tag{7}$$

where Q is the net transferred heat to external surface of target receiver as in Equation (8) and T_r is temperature.

$$Q = Q_{\mathrm{in}}{}^{*} - Q_{\mathrm{Loss}}, \tag{8}$$

where Q_{Loss} is the term used to describe the heat loss to temperature T_a and it changes based on the receiver setups. In the solar literature, the insulated pipes of nonevacuated with evacuated and cover glazing tubes are the two most common types of receivers to be encountered. The amount of heat that can be delivered to a receiver $Q_{\mathrm{in}}{}^{*}$ from a solar collector total mirror area is determined by three factors: direct sun radiation (DNI) on the mirror area A_m and the normal incidence $\eta_0(0=\theta)$ of the collector. The losses incurred by collectors are not taken into consideration in this computation as in the following equation:

$$Q_{\mathrm{in}}{}^{*} = \mathrm{DNI}.A_m\eta_0(0=\theta).\mathrm{IAM}. \tag{9}$$

In the calculation of optical efficiency and IAM, the following parameters are taken into consideration: reflectance, transmission, absorbance, intercept factor, shadowing, and blocking. Aspects such as the effective mirror aperture area and incidence cosines are also taken into consideration. In order to approximate the elevation of individual mirror elements, the following parameters must be known: the corresponding width (W), slope angle (θ_n), and shift (S_n) of the mirrors that are in operation and this helps in eliminating the shadowing es_n shown in the following equation:

$$es_n = \frac{W}{2}(\sin\theta_n + \sin\theta_{n+1}) - S_n\mathrm{Tan}\theta_p. \tag{10}$$

The height of the sun is often defined by the profile angle, denoted by p, which is the angle θ_p between the plane and sun vector that consists of the rotation axes of each mirror. It is important to note that this plane is perpendicular to the tracking axis of the mirror. The computations of the Sun-Earth geometry are not provided in this document. It is required to use an iterative procedure to estimate the correct slope angle when the elevation varies. Depending on the LFR design, a small separation between mirrors can cause reflected rays from surrounding mirrors to be obstructed. It is proposed that the following steps should be taken to remove blocking, and the equation is shown in the following:

$$eb_n = \frac{W}{2}(\sin\theta_{n+1} + \sin\theta_n) - \frac{S_n h}{(Q_{n+1} + (W/2)\mathrm{Cos}\theta_{n+1} + S_n)}, \tag{11}$$

where h is the receiver height and Q_n is the horizontal distance between the receiver tower and mirror element.

The LFR is biaxially dependent on the angle of direct sunlight incidence when viewed from different directions. Therefore, the transversal and longitudinal planes IAM (θ_t, θ_l) were employed in this work as angle modifiers for rays travelling in IAM(θ_t), which is the considered vertical plane and is found perpendicular to the axis of rotation, and IAM(θ_l), which is perpendicular to the rotation axes. When calculating biaxial IAMs, ray-tracing is frequently employed. IAM(θ_t) and IAM(θ_l) are used to compute the overall optical efficiency, which is the total of the transversal and longitudinal incidence angles of the sunbeams. IAM(θ_t) and IAM(θ_l) are used to determine the overall optical efficiency. The estimation of hourly stagnation temperatures, $T_{r,\max}$, is

made possible by an optical efficiency that is dependent on the incidence angle. The temperature reaches equilibrium when the amount of heat lost to the environment equals the amount of heat absorbed by the atmosphere and shown in the following equation.

$$T_{r,\max} = T_a + \frac{\mathrm{DNI}.\eta_0(\theta = 0).\mathrm{IAM}.A_m}{U_L A_r}, \tag{12}$$

where U_L is the coefficient of heat loss and A_r is the receiver area.

The heat loss coefficient is denoted by UL, while the receiver area is denoted by Ar. The captured radiation would be squandered if the stagnation temperature dropped below the desired operating temperature, as we anticipated. As a result, the collector has been rendered inoperable. Heat loss was estimated using a correlation of the parallel plate, which takes into account both convection and radiation heat losses from the receiver's bottom, together with conduction from the insulated sidewalls. Parallel plate correlation was used to estimate the heat loss. This results in a loss of the form Q_{Loss} equal to the following equation:

$$Q_{\mathrm{Loss}} = A_r U_L (T_r - T_a). \tag{13}$$

4.1. Classifier. An input layer I with a two-dimensional representation is followed by hidden convolution and pooling layers, as well as an output layer that is totally connected. Each convolution layer neuron has nonlinear kernels, which divide input into receptive fields as it passes through the layer. Following the completion of convolution at the k^{th} kernel in the l^{th} convolution layer, we can compute the following results in the following equation:

$$f_l^k(p, q) = \sum_c \sum_{x,y} i_c(x, y) e_l^k(u, v), \tag{14}$$

where $i_c(x, y) - (x, y)^{\mathrm{th}}$ is the element of channel c for I and $e_l^k(u, v) - (u, v)^{\mathrm{th}}$ is the element of kernel k for layer l.

Using a sweeping average or maximum function across tiny patches of convolution output, it is possible to avoid overfitting on the training set, resulting in an even lower dimension of the returned features. Finally, the fully connected layer establishes a connection between the collected features and the target label of the underlying classification or regression operation. The classifier is the circuit which produces the different heat source classification. Each convolution layer neuron has nonlinear kernels, which divide input into receptive fields as it passes through the layer. Based on this classification, the proposed model provides the quality optimization while compared with the existing models. In applications where local spatial and temporal correlations of data are important, the convolution and pooling layers of the CNN achieve state-of-the-art performance because they process their local input patches at the same time, a feature known as parallel processing. As a result, in real-world applications, our model outperforms SAE, ANNs, and LSTM models. By using a densely packed cell array to maximise electrical output, the LFR is less than 30 mm wide, which helps to maximise thermal efficiency. To maximise electrical output, the LFR is less than 30 mm broad. In addition to the kernel-based CNN utilised in the previous study, recent research has developed spectral graph convolutions to capture spatial patterns in graph-structured power system datasets. The convolution operation of the graph CNN is computed for an N-node graph with D -dimensional features $X \in R^{N \times D}$, adjacency matrix A, and degree matrix D in the following equation:

$$f(X, A) = \sigma\left(D^{-0.5} A D^{-0.5} X W\right), \tag{15}$$

where W is the weighted matrix at the convolution layer.

The linear Fresnel reflector was constructed and produces the quality solar tracking in the north-south direction. So the solar light energy optimization will increase due to these activities. There is also no mirror placed beneath the absorber to prevent the shadow generated by this device and the secondary concentrator.

5. Results and Discussions

The results of the proposed LRF with existing models are shown between Figures 2–5. The Analytical Hierarchy Process (AHP) was used to handle the issue of assigning importance to client needs in QFD research, which was previously addressed by other methods (AHP). For concept design modifications to be evaluated against consumer and technical criteria as well as their priorities while using an AHP framework, the addition of a Pugh matrix must be made to the framework. It is a difficult technique to execute an AHP, QFD, and Pugh matrix combination because of their interdependence. When used together, QFD and AHP are complementary strategies that can be utilised to aid in the prioritisation of technical difficulties. This will not be accomplished just through the use of the Pugh matrix. As a result, the more difficult technique was able to discern between the different notions. The researchers emphasised that they had a 15% preference for the Elevation Linear Fresnel Reflector (ELFR) design over the circular method in their study. Here, the Matlab is the simulation tool used to compute the performance of the proposed model. This tool is used to gather the results and help to compare the proposed model with the existing models. An often-heard criticism of quantitative factor analysis and adaptive hypothesis testing is that the results can be highly dependent on the criteria that are used in the procedure. As a result of this selection, various models emerge as the greatest. To address this issue, thorough technical and economic research, as well as comparisons with existing LFR designs, has been carried out.

The improved performance of the LFR can be observed immediately after installation. The LFR increases energy consumption by 13%, adds 274 additional operating hours per year, and reduces land use by 17% by keeping the working temperature at 300°C all year. The H-variable arrangement, which is a layout of horizontal mirror spacing specified for shadowing at a sun transverse angle of 45°, is an improvement when compared to the present

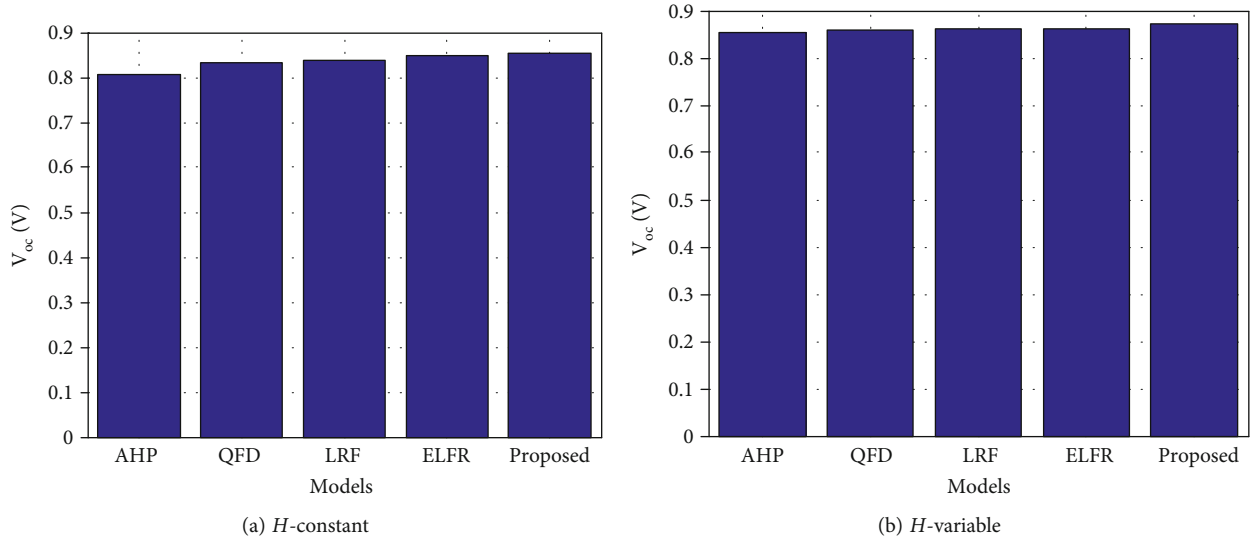

(a) *H*-constant (b) *H*-variable

Figure 2: Variances in open-circuit voltage.

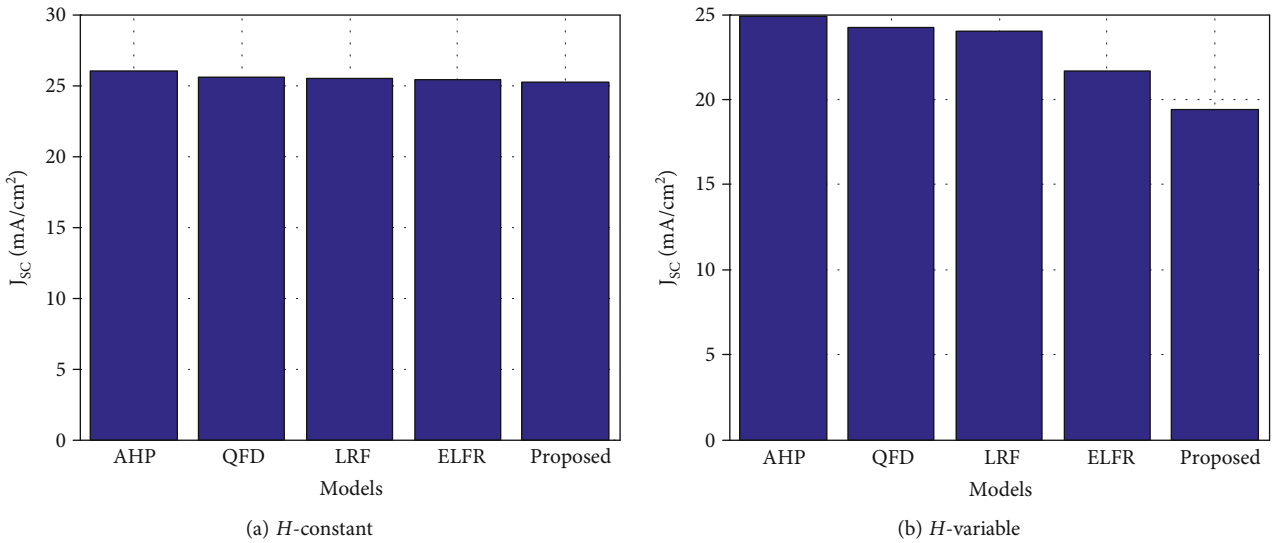

(a) *H*-constant (b) *H*-variable

Figure 3: Short circuit current.

arrangement. The energy increase over a standard narrow constant horizontal mirror spacing configuration, denoted by the *H*-constant, is predicted to be 23%. The annual optical efficiency of the LFR is expected to be 49%, compared to 39% for the H-constant models. These figures are equal when compared to the annual optical efficiency of the Fresdemo LFR, which is 43% every year. Even though the LFR has certain potential financial drawbacks, it is still worth investigating. The cost per unit of energy increases by 2% and 6% for *H* -constant due to the cost associated with elevating components. In a scenario with high land costs, the cost per unit of energy for the LFR would be reduced by 60% if component costs were reduced by 60% compared to the *H*-constant.

The design that is most appropriate for a given situation will be dictated by the priorities that have been established. The LFR has the potential to be extremely beneficial, when additional factors are taken into consideration, effective land use becomes even more advantageous. Solar thermal power plants will benefit from higher temperatures for longer periods during the day, increasing the number of full load hours and the amount of storage available. Major modifications are required for an electricity-producing plant that uses ELFRs to overcome the system's rising capital costs and increasing complexity. The utilisation of more detailed source data can be utilised to develop more advanced forecasting models, which can then be used to attain an increased average accuracy rate of PV power forecasts. This was improving the use of minimum utilisation while the power forecasting was dry. The constraints of the LFR must be addressed, and the cost-effectiveness of the technology must be enhanced. To keep the cost and complexity of the prototype as low as possible, the team developed serial

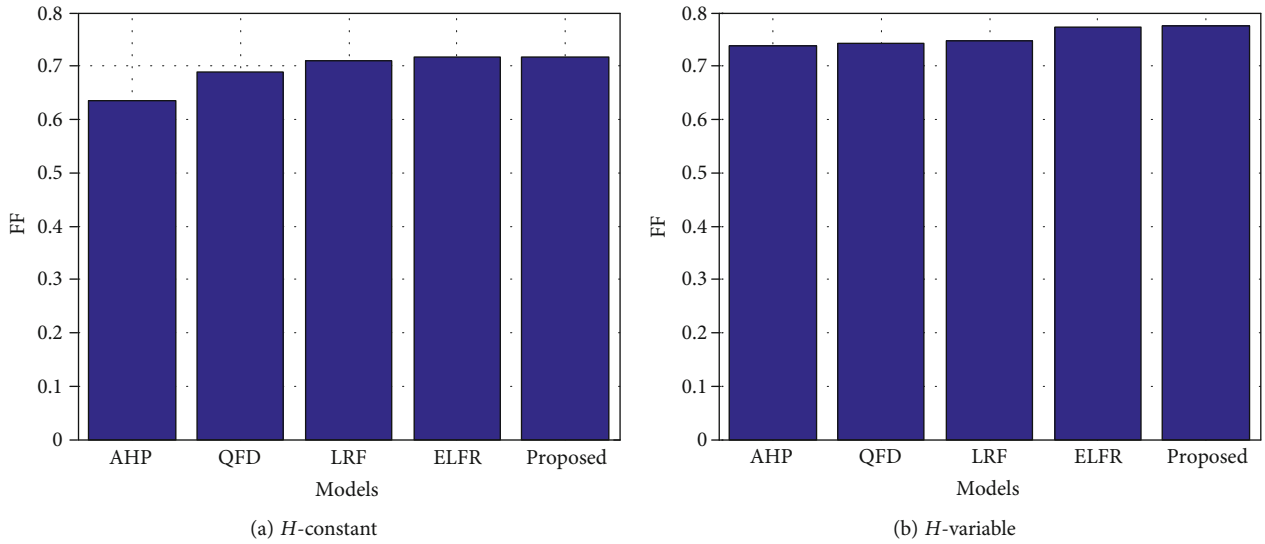

(a) H-constant (b) H-variable

Figure 4: Fill factor.

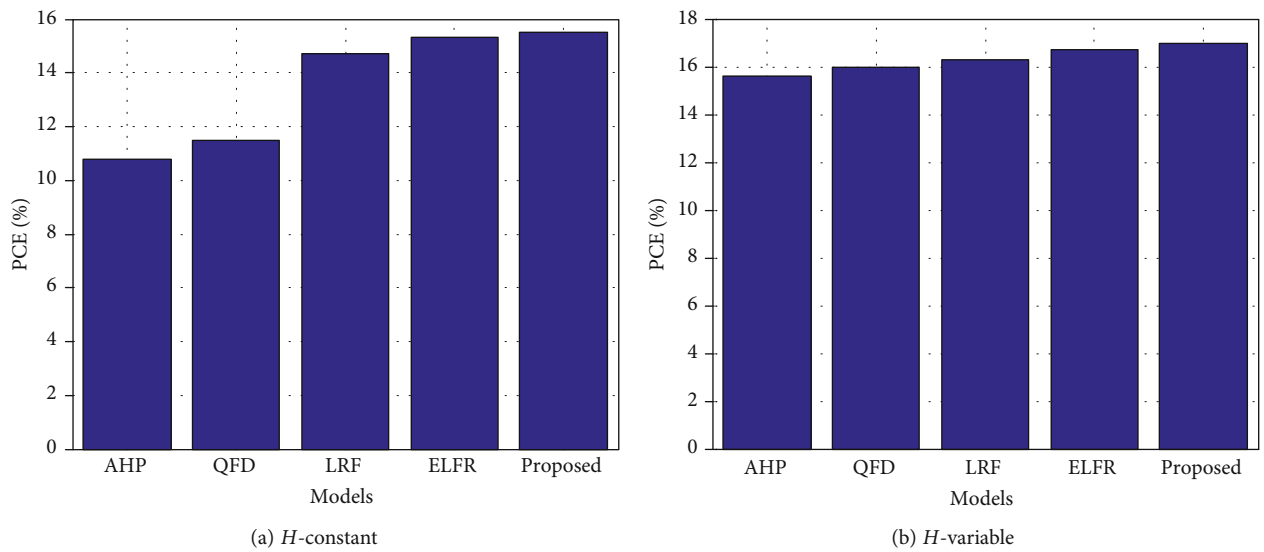

(a) H-constant (b) H-variable

Figure 5: Power conversion efficiency.

communication boards that ease control while minimising cabling and auxiliary power demands. The adoption of embedded control systems in large-scale installations would be advantageous because it would make things even easier to manage. The tracking of solar lights was too important to optimize the power in various proposed methods. The computation of the different methods getting the motor rotation on solar light tracking is slightly less than the proposed model predictions. The proposed model analyzes the high power location and time in the smart machine leaning method. So the proposed model gets more results compared with the other existing models.

6. Conclusions

In this paper, we study the distributed rooftop solar, i.e., LFR performance. LFR can take advantage of some of their most significant advantages, such as the removal of transmission losses and the generation of electricity at the point of sale. Concentrated solar power technology, on the other hand, is a realistic option when it comes to achieving ever-lower normalised energy costs and ever-shorter energy payback times. For CPV applications, materials, components, and manufacturing techniques from the power electronics sector, in particular, have been adapted to lower system costs and time to market, as well as to improve system performance and reliability. As a result of using a densely packed cell array to maximise electrical output, the LFR is less than 30 mm wide, which helps to maximise thermal efficiency. To maximise electrical output, the LFR is less than 30 mm broad. The Matlab simulations suggest that the proposed machine learning-based LFR technique has a higher concentration rate than the current LFR technique, which is supported by the results of the experiment.

Data Availability

The data used to support the findings of this study are included within the article. Further data or information is available from the corresponding author upon request.

Conflicts of Interest

The authors declare that there are no conflicts of interest regarding the publication of this paper.

Acknowledgments

The authors appreciate the supports from Arba Minch University, Ethiopia, for the research and preparation of the manuscript. The authors thank Velammal Engineering College, MJP Rohilkhand University, and Vel Tech Rengarajan Dr. Sagunthala R&D Institute of Science and Technology for providing assistance to this work.

References

[1] O. Erixno, N. Abd Rahim, F. Ramadhani, and N. N. Adzman, "Energy management of renewable energy-based combined heat and power systems: a review," *Sustainable Energy Technologies and Assessments*, vol. 51, article 101944, 2022.

[2] E. W. Ramde, E. T. Tchao, Y. A. K. Fiagbe, J. J. Kponyo, and A. S. Atuah, "Pilot low-cost concentrating solar power systems deployment in sub-Saharan Africa: a case study of implementation challenges," *Sustainability*, vol. 12, no. 15, p. 6223, 2020.

[3] M. E. Zayed, J. Zhao, A. H. Elsheikh, W. Li, S. Sadek, and M. M. Aboelmaaref, "A comprehensive review on dish/Stirling concentrated solar power systems: design, optical and geometrical analyses, thermal performance assessment, and applications," *Journal of Cleaner Production*, vol. 283, article 124664, 2021.

[4] S. Wu, C. Wang, and R. Tang, "Optical efficiency and performance optimization of a two-stage secondary reflection hyperbolic solar concentrator using machine learning," *Renewable Energy*, vol. 188, pp. 437–449, 2022.

[5] A. Latif, S. S. Hussain, D. C. Das, and T. S. Ustun, "State-of-the-art of controllers and soft computing techniques for regulated load frequency management of single/multi-area traditional and renewable energy based power systems," *Applied Energy*, vol. 266, article 114858, 2020.

[6] R. Uthirasamy, V. Kumar Chinnaiyan, S. Vishnukumar et al., "Design of boosted multilevel DC-DC converter for solar photovoltaic system," *International Journal of Photoenergy*, vol. 2022, Article ID 1648474, 23 pages, 2022.

[7] Z. D. Cheng, X. R. Zhao, Y. L. He, and Y. Qiu, "A novel optical optimization model for linear Fresnel reflector concentrators," *Renewable Energy*, vol. 129, pp. 486–499, 2018.

[8] H. S. Dhiman and D. Deb, "Fuzzy TOPSIS and fuzzy COPRAS based multi-criteria decision making for hybrid wind farms," *Energy*, vol. 202, article 117755, 2020.

[9] Z. Zeng, D. Ni, and G. Xiao, "Real-time heliostat field aiming strategy optimization based on reinforcement learning," *Applied Energy*, vol. 307, article 118224, 2022.

[10] A. Khosravi, M. Malekan, J. J. G. Pabon, X. Zhao, and M. E. H. Assad, "Design parameter modelling of solar power tower system using adaptive neuro- fuzzy inference system optimized with a combination of genetic algorithm and teaching learning-based optimization algorithm," *Journal of Cleaner Production*, vol. 244, article 118904, 2020.

[11] A. P. Gonzalo, A. P. Marugán, and F. P. G. Márquez, "Survey of maintenance management for photovoltaic power systems," *Renewable and Sustainable Energy Reviews*, vol. 134, article 110347, 2020.

[12] H. A. Maddah, M. Bassyouni, M. H. Abdel-Aziz, M. S. Zoromba, and A. F. Al-Hossainy, "Performance estimation of a mini-passive solar still _via_ machine learning," *Renewable Energy*, vol. 162, pp. 489–503, 2020.

[13] C. Liu, Q. Ma, Z. J. Luo et al., "A programmable diffractive deep neural network based on a digital-coding metasurface array," *Nature Electronics*, vol. 5, no. 2, pp. 113–122, 2022.

[14] X. Fu, Y. Zhou, F. Yang et al., "A review of key technologies and trends in the development of integrated heating and power systems in agriculture," *Entropy*, vol. 23, no. 2, p. 260, 2021.

[15] R. Pirayeshshirazinezhad, S. G. Biedron, J. A. D. Cruz, S. S. Guitron, and M. Martínez-Ramón, "Designing Monte Carlo simulation and an optimal machine learning to optimize and model space missions," *Access*, vol. 10, pp. 45643–45662, 2022.

[16] N. Yuvaraj, K. Praghash, R. A. Raja, and T. Karthikeyan, "An investigation of garbage disposal electric vehicles (GDEVs) integrated with deep neural networking (DNN) and intelligent transportation system (ITS) in smart city management system (SCMS)," *Wireless Personal Communications*, vol. 123, no. 2, pp. 1733–1752, 2022.

[17] M. Hasan, M. Warburton, W. C. Agboh et al., "Human-like planning for reaching in cluttered environments," in *2020 IEEE International Conference on Robotics and Automation (ICRA)*, pp. 7784–7790, Paris, France, 2020, May.

[18] Z. Tong, J. Cai, J. Mei, K. Li, and K. Li, "Dynamic energy-saving offloading strategy guided by Lyapunov optimization for IoT devices," *IEEE Internet of Things Journal*, 2022.

[19] A. Kumar, G. Wu, M. Z. Ali, R. Mallipeddi, P. N. Suganthan, and S. Das, "A test-suite of non-convex constrained optimization problems from the real- world and some baseline results," *Swarm and Evolutionary Computation*, vol. 56, article 100693, 2020.

[20] S. Ghimire, R. C. Deo, H. Wang, M. S. Al-Musaylh, D. Casillas-Pérez, and S. Salcedo-Sanz, "Stacked LSTM sequence-to-sequence autoencoder with feature selection for daily solar radiation prediction: a review and new modeling results," *Energies*, vol. 15, no. 3, p. 1061, 2022.

[21] A. Peloni, A. V. Rao, and M. Ceriotti, "Automated trajectory optimizer for solar sailing (atoss)," *Aerospace Science and Technology*, vol. 72, pp. 465–475, 2018.

[22] C. Feng, J. Zhang, W. Zhang, and B. M. Hodge, "Convolutional neural networks for intra-hour solar forecasting based on sky image sequences," *Applied Energy*, vol. 310, article 118438, 2022.

[23] M. Premkumar, P. Jangir, C. Ramakrishnan, G. Nalinipriya, H. H. Alhelou, and B. S. Kumar, "Identification of solar photovoltaic model parameters using an improved gradient-based optimization algorithm with chaotic drifts," *IEEE Access*, vol. 9, pp. 62347–62379, 2021.

[24] B. Gobinathan, M. A. Mukunthan, S. Surendran et al., "A novel method to solve real time security issues in software industry using advanced cryptographic techniques," *Scientific Programming*, vol. 2021, Article ID 3611182, 9 pages, 2021.

[25] Z. L. Li, P. Li, Z. P. Yuan, J. Xia, and D. Tian, "Optimized utilization of distributed renewable energies for island microgrid clusters considering solar-wind correlation," *Electric Power Systems Research*, vol. 206, article 107822, 2022.

[26] X. Xu, Z. Wei, Q. Ji, C. Wang, and G. Gao, "Global renewable energy development: influencing factors, trend predictions and countermeasures," *Resources Policy*, vol. 63, article 101470, 2019.

[27] N. Yuvaraj, K. Praghash, and T. Karthikeyan, "Data privacy preservation and trade-off balance between privacy and utility using deep adaptive clustering and elliptic curve digital signature algorithm," *Wireless Personal Communications*, vol. 2021, article 3611182, pp. 1–16, 2021.

[28] J. Gao, H. Wang, and H. Shen, "Smartly handling renewable energy instability in supporting a cloud datacenter," in *2020 IEEE international parallel and distributed processing symposium (IPDPS)*, pp. 769–778, IEEE, 2020.

[29] L. L. Li, S. Y. Wen, M. L. Tseng, and C. S. Wang, "Renewable energy prediction: a novel short-term prediction model of photovoltaic output power," *Journal of Cleaner Production*, vol. 228, pp. 359–375, 2019.

[30] F. Rodríguez, A. Fleetwood, A. Galarza, and L. Fontán, "Predicting solar energy generation through artificial neural networks using weather forecasts for microgrid control," *Renewable Energy*, vol. 126, pp. 855–864, 2018.

[31] M. Sharif, J. Amin, M. Raza, M. Yasmin, and S. C. Satapathy, "An integrated design of particle swarm optimization (PSO) with fusion of features for detection of brain tumor," *Pattern Recognition Letters*, vol. 129, pp. 150–157, 2020.

[32] S. S. Band, S. Janizadeh, S. Chandra Pal et al., "Novel ensemble approach of deep learning neural network (DLNN) model and particle swarm optimization (PSO) algorithm for prediction of gully erosion susceptibility," *Sensors*, vol. 20, no. 19, p. 5609, 2020.

[33] C. K. H. Lee, "A review of applications of genetic algorithms in operations management," *Engineering Applications of Artificial Intelligence*, vol. 76, pp. 1–12, 2018.

[34] T. Harada and E. Alba, "Parallel genetic Algorithms," *ACM Computing Surveys (CSUR)*, vol. 53, no. 4, pp. 1–39, 2021.

[35] S. Alseekh, A. Aharoni, Y. Brotman et al., "Mass spectrometry-based metabolomics: a guide for annotation, quantification and best reporting practices," *Nature Methods*, vol. 18, no. 7, pp. 747–756, 2021.